IN-FLIGHT MEASUREMENT AND CORRECTION OF NON-LINEARITY OF THE POLDER-1's SENSITIVITY

Bertrand FOUGNIE, Olivier HAGOLLE, François CABOT

Centre National d'Etudes Spatiales (CNES)
18,avenue Edouard Belin - 31401 Toulouse CEDEX 4-France – Bertrand.Fougnie@cnes.fr

RESUME – Un défaut de non-linéarité de la sensibilité de capteur POLDER-1 a pu être détecté à l'aide d'images acquises au dessus des sites désertiques. Ce papier présente la méthode de mesure de ce défaut, le modèle qui a pu être établi, la méthode de correction appliquée et l'impact sur la qualité des produits POLDER. Les performances de linéarité de l'instrument sont, après correction meilleurs que 1%.

ABSTRACT- *Using POLDER 1 in-flight measurements over desert sites, a non-linearity defect the instrument's sensitivity has been detected. This paper presents the measurement method, the defect model and the correction method, as well as the consequences on POLDER products. The linearity performances after correction are now better than 1%.*

1 - INTRODUCTION

Measuring the linearity of satellite borne optical instruments in the visible part of the electromagnetic spectrum is a task that has to be conducted with a special care since it requires to perform several absolute calibrations with different levels of radiance. Even if some error sources introduce constant biases whatever the radiance is, it is not easy to ensure a 1% performance when usual absolute calibration errors are greater than 3%. Non-linearity measurement are already difficult when performed in the laboratory, but they often become impossible after launch, and usually the in-flight linearity performance is assumed to be the same as the one measured prior to the launch. However, some instruments calibration teams (OCTS,[1]; SPOT3) have detected non-linearity differences among the detectors in CCD linear arrays that observe the same spectral bands, but these were relative measurements that only enable to detect elementary detectors that have a non-linearity different from the average non-linearity of the array.
For POLDER 1, an absolute non-linearity measurement has been possible in-flight, thanks to two important features : POLDER instrument has two different channels that correspond to the same spectral band (443 nm), and it is possible to program acquisitions with different integration times. Comparing the output from the two 443 channels over stable desert sites, a model of POLDER non-linearity is derived and then corrected in the level 1 processing.

2 - THE POLDER INSTRUMENT

POLDER 1 (POLarization and Directionality of Earth Reflectances) is a CNES instrument on-board NASDA's ADEOS 1 (ADvanced Earth Observing Satellite) polar orbiting satellite, which was successfully launched in August 1996. On the 30th of October 1996, POLDER 1 entered its nominal acquisition phase and worked perfectly until ADEOS early end of service on June the 30th 1997. A second POLDER instrument, identical to POLDER 1 will be launched with the ADEOS 2 satellite. POLDER is a multi-spectral imaging radiometer/polarimeter designed to collect global and repetitive observations of the solar radiation reflected by the Earth/Atmosphere System, with a wide field of view (2400 km) and a moderate geometric resolution (6 km). The instrument concept is based on a matricial CCD array that can perform measurements in eight spectral bands, thanks to a

rotating wheel carrying spectral filters. POLDER has also a unique ability to measure polarized reflectances using three polarizers (for three of its nine spectral bands), and to observe target reflectances from 13 different viewing directions during a single satellite pass.
The POLDER instrument is deeply described in [2] and [3]. It is made of three main features : a CCD array detector, a rotating wheel carrying spectral filters and polarizers, and wide field of view telecentric optics. The optics have a focal length of 3.57 mm, opening to f/4.5 with a maximum field of view of 114°. The CCD sensor array is composed of 242 x 274 independent sensitive areas and the nadir geometric resolution is 6 x 7 km. The rotating wheel rotates steadily with a period of 4.9 s and carries the interference filters and polarizers that select the spectral band and polarization direction. It carries 16 slots, including an opaque filter to estimate the CCD detector dark current. The remaining 15 slots carry 6 unpolarized and 9 polarized filters (3 polarization directions for 3 different wavelengths). Thus, POLDER acquires measurements in 9 bands, 3 of them are polarized.

2.1 - Spectral bands

POLDER has 9 spectral bands ranging from 443 nm to 910 nm. In Table 1, the nine bands are defined by their central wavelength, spectral width and polarization capability (channels having a polarization capability are identified by a P added to the wavelength number (ex : 443P)). As stated in the introduction, POLDER has two different 443nm spectral channels, because the presence of a polarizer reduces the radiance that arrives on the CCD array, it was not possible to meet the noise requirements necessary for ocean color mission with the 443P channel where the silicon sensitivity is already very low [2]. A second 443 nm channel (443NP for Not Polarized) has been added to measure the radiance without polarizers, and thus with a better signal to noise ratio. This feature has been intensively used to monitor POLDER image quality by comparing the radiances observed by both spectral bands, and was used to discover the non-linearity defect.

POLDER band name	443P	443NP	490	565	670P	763	765	865P	910
Central Wavelength (nm)	444.5	444,9	492.2	564.5	670.2	763.3	763.1	860.8	907.7
Band Width (nm)	20	20	20	20	20	10	40	40	20
Polarization	Yes	No	No	No	Yes	No	No	Yes	No

Table 1 – POLDER spectral bands.

2.2 - Dynamic range

The CCD array sensitivity varies a lot with the wavelength, beginning at around 5% at 443 nm, up to 35% at 670 nm, and back to 10% at 900 nm. But the solar radiation also varies by nearly a factor 2 between 443 and 910 nm, the polarizers can absorb 50% of the light and POLDER various missions require different dynamic ranges. Since a single CCD array is used for all the spectral bands, it has been necessary to equilibrate the radiances arriving on the CCD so that the tensions coming out of the CCD have the same dynamic range. To do that, optical attenuating filters have been used to reduce the output of the CCD for some spectral bands, but also a degree of freedom has been obtained by the ability to use two different integration time according to the spectral band (Table 2).

Short Integration Time (SIT)	23.76 ms
Long Integration Time (LIT)	105.137 ms

Table 2 – POLDER integration time.

The nominal plan for the attribution of integration times to the spectral bands varied a lot during POLDER 1 development. At the beginning [2], the idea was to attribute a LIT to all the spectral bands used exclusively by ocean color mission (443NP, 490, 565) . With this programming, the clouds would be saturated, but the ocean surface would be seen with a better signal to noise ratio. Later on, it appeared that a stray-light correction was necessary and could not be well corrected if a lot of pixels were saturated. That's why, the standard programming of 490 and 565 nm was set to SIT. 443NP was programmed with LIT because it is possible to retrieve the exact values from 443P for the stray-light correction. However, some phases in the commissioning phase required to use the SIT and during Polder life, this spectral band was alternatively programmed in SIT and LIT (Table 3). At the end of POLDER calibration phase (May 97), SIT and LIT values were increased by 10% to optimize the dynamic range, but unfortunately, the ADEOS satellite failed a few days later (June 30th, 1997).

POLDER band	443P	443NP	490	565	670P to 910
Standard programming sequence	LIT	LIT or SIT	SIT	SIT	SIT
Saturation level (normalized radiance)	1.1	0.22 or 0.97	0.75	0.48	1.1

Table 3 – POLDER programming of integration times and related saturation levels expressed in normalized radiance.

2.3 - Level 1 processing

In POLDER level 1 products, the data are geolocated and calibrated. For the polarized spectral bands, the combination of the measurements in three polarization directions allows to retrieve the 3 first components of the Stokes vector, the fourth component that characterizes the ellipticity of polarization being very close to zero. The first component of the Stokes vector I, is the total radiance (ie Unpolarized radiance + Polarized radiance). In POLDER level 1 products, it is expressed as a normalized radiance :

$$I = \pi. \text{ Radiance / Solar irradiance} = \text{reflectance} * \cos(\text{sun zenith Angle}) \quad \text{(Eq. 1)}$$

The radiometric model of POLDER is rather complicated (it is detailed in [4]), but after all the corrections performed in the level 1 processing to account for polarization inversion and various sensor artefacts, it can be simplified as follows :

$$DN_k(t) = A_k .t . I_k \quad \text{(Eq. 2)}$$

Where, for the spectral band k, DN_k is the digital number measured by the instrument for spectral band k and corrected from the dark current, A is the absolute calibration coefficient, t is the integration time, and I_k is the total radiance. This radiometric model is called "linear" because DN is directly proportional to the radiance I. A detailed description of POLDER level 1 processing is given in *[4]*). As a result of level 1 processing, the differences between the total radiance measured by 443P or 443NP should be very small. The main error sources are :

- geometrical registration error (less than 0.2 pixel) and interpolation
- instrument noise
- slight difference in spectral response of 443P and 44NP (0.4 nm in Table 1).

However, using spatially uniform sites, the two first error sources vanish and comparison of total radiances measured in both 443P and 443NP spectral bands should give very close results.

3 - EVIDENCE OF A NON-LINEARITY DEFECT

3.1 - Desert sites

Stable desert areas of Sahara and Saudi Arabia are often used as calibration test sites in the solar reflected spectrum. Such sites have already been used to monitor the calibration temporal drifts of the AVHRR and METEOSAT [5], ATSR-2 [6], and HRV/SPOT sensors[7]. They can also be used to estimate the multi-angular calibration of wide field of view sensors such as POLDER as shown in*[8]*. A procedure has been defined to select 100x100 km² desert areas in North Africa and Saudi Arabia [9], using a spatial uniformity criterion in Meteosat-4 visible data. Twenty such sites meet this criterion within 3%. The temporal stability of the spatially averaged reflectance of each selected site has been investigated at seasonal and hourly time scales with multi-temporal series of Meteosat-4 data. It was found that the temporal variations, typically 8-15% peak-to-peak in relative value, were mostly controlled by directional effects. Once the directional effects are removed, the residual root mean square variations, representative of random temporal variability, are in the order of 1-2% in relative values. All the POLDER acquisitions over any of the 20 desert sites have been compiled in a data base that contains the angular conditions and the radiances, averaged over the site, for each POLDER spectral band. This data base is used for the multi-angular calibration of POLDER and to cross calibrate POLDER to other optical instruments [10].

3.2 - Defect evidence

Plotting the ratio of 443P and 443NP total radiance measured over desert sites, as a function of time (Figure 1), we observed sudden drops of the ratio occurring at some very precise dates. The explanation of the phenomenon came quickly as we discovered that the dates of the drops were the dates when the integration time of 443NP passed from SIT value to LIT value. The average difference of the ratio of 443P and 443NP measurements over desert sites, during SIT periods and LIT periods is about 1.4%.

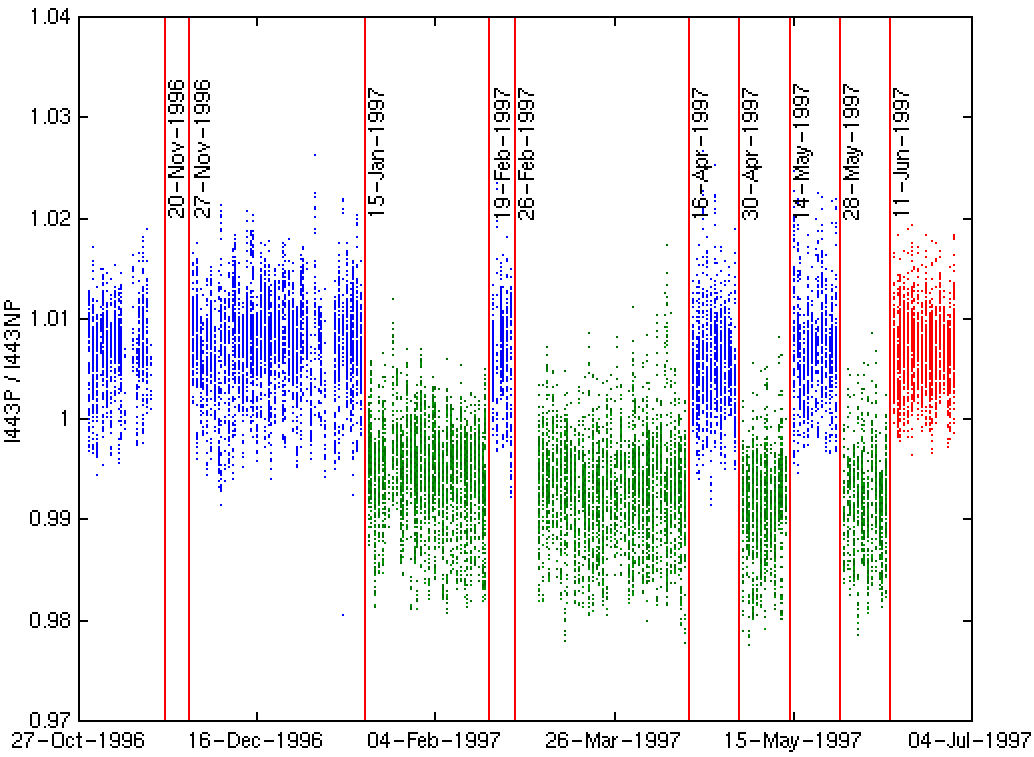

Figure 1 – I443P / I443NP as a function of time. The 443P band is always programmed in LIT while the 443NP band is alternatively programmed in SIT (up) and LIT (down).

An explanation by a natural evolution of the desert sites can obviously be rejected, and the coincidence with the change in integration times shows that the origin of the problem lies in POLDER electronics. Three hypotheses could be suggested :

- the exact value of integration time is not exactly what is expected
- the instrument output has an offset depending on the integration time
- the instrument gain is not perfectly linear

We call hereafter I_k[LIT] and I_k[SIT], the radiance observed for the spectral band k and respectively for long and short integration times. In order to characterize this defect, we have plotted the value of $\left\langle \frac{I_{443P}[LIT]}{I_{443NP}[SIT]} \right\rangle \Big/ \left\langle \frac{I_{443P}[LIT]}{I_{443NP}[LIT]} \right\rangle$ as a function of $I_{443P}[LIT]$, i.e. as a function of the observed radiance. This ratio is nearly equal to $\frac{I_{443NP}[LIT]}{I_{443NP}[SIT]}$ if we assume that the spectral shape of the observe targets does not vary between the SIT periods and the LIT periods. Figure 2 shows an increase of this ratio in the range of radiance available over desert sites (typically 0.1 < I_{443P}[LIT] <0.23). If the first hypothesis was true, the ratio should have a constant value, and if the second hypothesis was true, the ratio should decrease. This curve thus confirms the third hypothesis, i.e. a non linearity of the instrument gain.

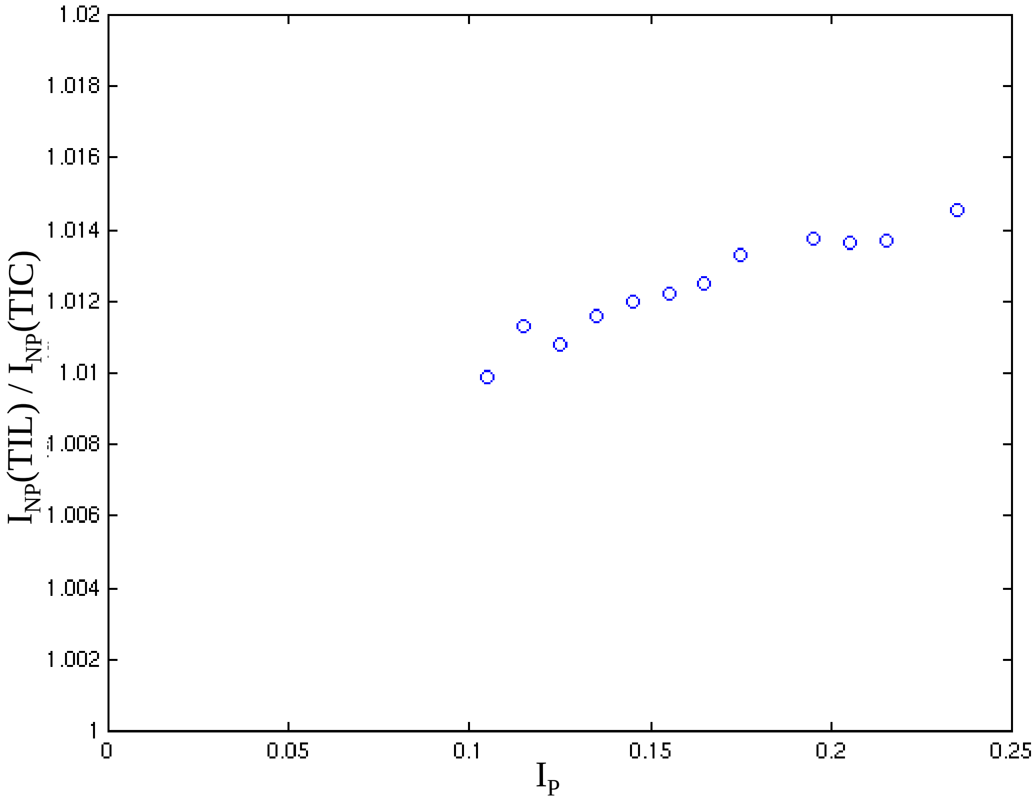

Figure 2 – Discrepancy between radiances measured with SIT and LIT, as a function of radiance.

4 - DEFECT MODELING

We have seen in the previous paragraph that the non-linearity depends on the radiance and on the integration time. If it was only a function of the radiance, no discrepancy would be seen on Figure 1. Thus, our basic hypothesis is that the non linearity occurs at the output of the array or beyond in the electronics, and that it can be expressed as a function of the digital numbers delivered by the instrument. Since POLDER 1 sensitivity appears to be not linear, the radiometric model must be changed. Contrarily to Eq. (2) where DN was simply proportional to I, the digital number is now a function of the radiance I and can be expressed as

$$DN_k(t) = f\,(\,A_k\,.t\,.\,I_k\,) \qquad \text{(Eq. 3)}$$

This function, hereafter called "f", is obviously more complicated than the linear function. The initial value f(0) is 0 since the digital numbers are corrected from the dark current. The first consequence of this is that the behavior illustrated Figure 2 is more exactly the variation of $\frac{DN_{443NP}(t_{LIT})}{DN_{443NP}(t_{SIT})}$ with $DN_{443P}(t_{SIT})$. The second consequence is that this relationship, called F, can be written using Eq. (3) as

$$\frac{DN_{443NP}(t_{LIT})}{DN_{443NP}(t_{SIT})} = \frac{f(A_{443NP}.I.t_{LIT})}{f(A_{443NP}.I.t_{SIT})} = F(DN_{443P}(t_{SIT})) = F(f(A_{443P}.I.t_{SIT})) \qquad \text{(Eq. 4)}$$

This equation has been solved numerically assuming f(x) can be expressed as a 2nd order polynomial of $\sqrt{x}$. Figure 3 illustrates the discrepancy between the POLDER radiometric model including the non linearity defect correction (using the f function) and a perfectly linear radiometric model. For this, the calibration coefficient is supposed computed for radiances corresponding to digits close to 350.

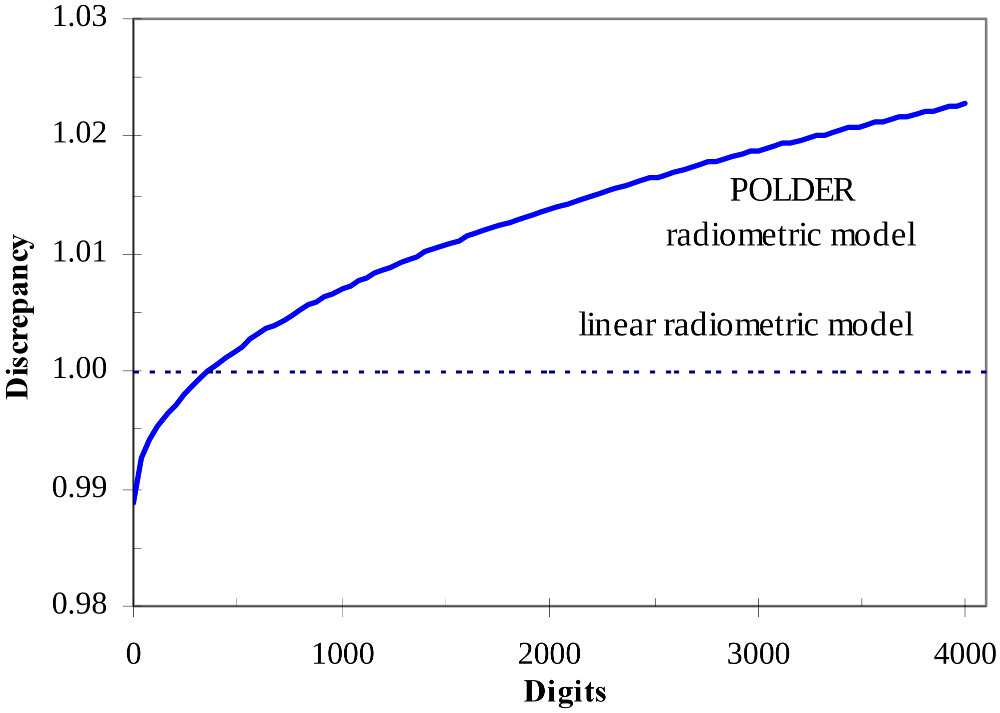

Figure 3 – Discrepancy between the POLDER radiometric model and a perfectly linear radiometric model.

Even if the discrepancy noted in Figure 1 is about 1.5%, the overall non linearity over the whole dynamic range (from 0 to saturation) reaches 3%. Because all the POLDER spectral bands are acquired by the same CCD array and since the defect seems to be located in the electronic chain (i.e. after the CCD), our hypothesis is that the f function can be generalized whatever the spectral band.

Finally, using Eq. (3), the radiance can be written for all the POLDER pixels and whatever the wavelength as

$$I_k = \frac{f^{-1}(DN_k(t))}{A_k \cdot t} \qquad \text{(Eq. 5)}$$

and the correction can be applied to POLDER data.

5 - MODEL VALIDATION

5.1 - Validation over desert sites

The non linearity model previously elaborated has been used to correct the desert site data plotted in Figure 1 which is re-plotted in Figure 4. No residual bias greater than 0.5% is found all over the POLDER life and whatever the integration time and this value can be considered as the accuracy of the non linearity defect correction. The limitation of this result is that only the correction for the 443 spectral band is validated.

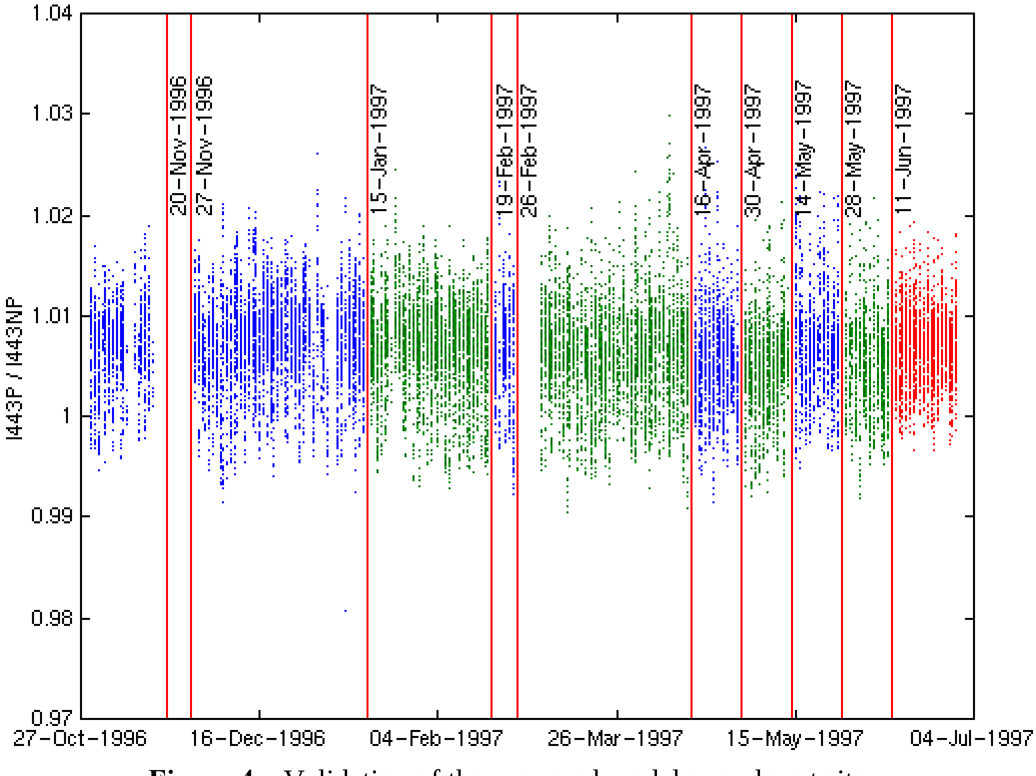

Figure 4 – Validation of the proposed model over desert sites.

5.2 - Validation over Rayleigh scattering

It has been explained and shown in table 3. that the spectral bands 490 and 565 nm were programmed with SIT because of some saturation problems. In fact, one exception occurred for only one week in February 1997 (from 02/26/97 to 03/04/97 included) for which these two bands were programmed with LIT in addition to 443. The opportunity to extend our validation to two other spectral band (and by extrapolation to all spectral bands) was then offered using the Rayleigh scattering method, the only natural target which did not lead to saturation for LIT. The absolute calibration method over Rayleigh scattering, detailed for POLDER in *[8]*, has been applied. In this method, the radiance observed by the satellite (DN_k / (A_k t)) is compared to the a reference radiance computed for the same geometric and atmospheric conditions in order to monitor some possible evolution, called ΔA_k, on the radiometric calibration coefficient A_k. Here, the idea is to compute the ΔA_k using the POLDER level-1 data, not corrected by the non-linearity effect, for two different acquisition time (SIT and LIT) and to try to identity the non-linearity defect. For this, we use POLDER acquisitions over 4 oceanic sites in Pacific and Atlantic oceans *[8]*, for the week in LIT and for its previous and following weeks in SIT. As the absolute accuracy of the Rayleigh scattering method is only a few percents for these wavelengths, it was only possible to observe the non linearity as a relative effect between acquisitions in TIL and TIC. Consequently, for each of the oceanic sites, the A_k coefficient found in the LIT conditions (2 weeks) was normalized by the A_k coefficient found in the SIT conditions (1 week). Figure 5, the mean variation of A_k values derived from SIT and LIT acquisitions were reported on the curve of the Figure 3. The value derived from SIT (near digits 300) was adjusted on the curve deduced from our model and the corresponding mean evolution found for the LIT acquisitions (near digits 1500) is shown. If the results appeared noisy for 443nm as previously observed in *[8]*, the discrepancy found for the LIT acquisitions is consistent within ±1% for these 3 wavelengths with the proposed non linearity model.

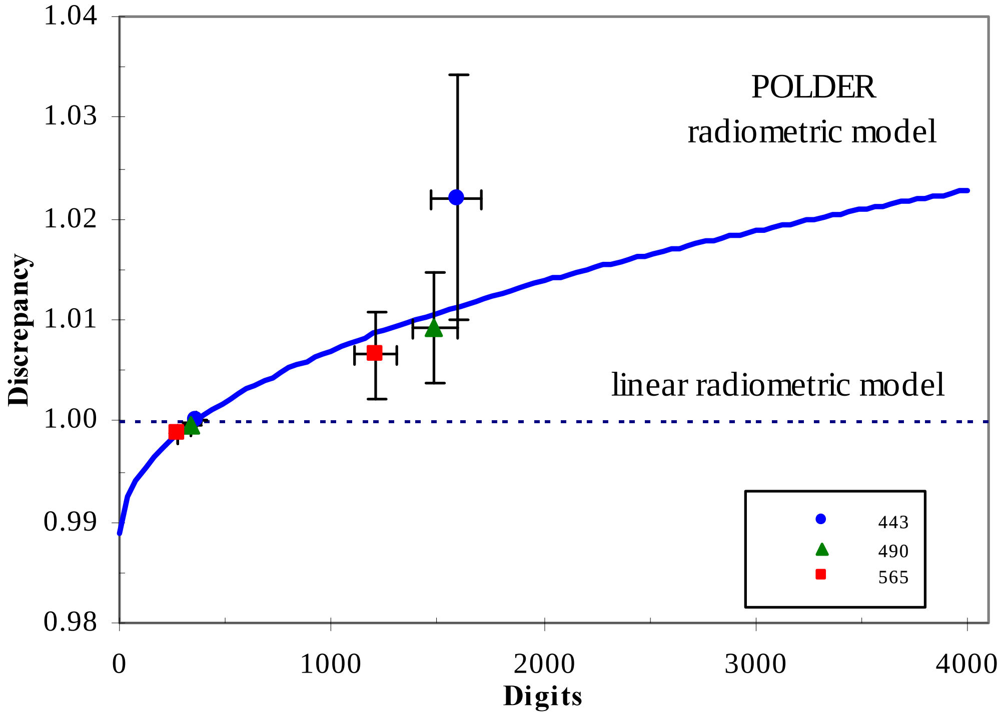

Figure 5 – Validation of the proposed model over Rayleigh scattering. Error bars are standard deviations of the digits/calibration coefficients over the 4 sites and the 2 weeks.

CONCLUSION

A non linearity defect was identified in the POLDER-1 sensitivity thanks to ratio derived from measurements in both polarized and non-polarized spectral bands at 443nm. A defect model is proposed and the effects of linearity is found to be about 3% from min to max over all the dynamic range. The proposed model was validated using acquisitions over desert and oceanic sites. Some scientific products derived from POLDER-1 measurements, mainly ocean color products for which sensor calibration is a critical topic, are sensitively impacted by this non linearity problem which leads for example to erroneous multi-temporal variations. Consequently, after a necessary reprocessing of the POLDER-1 calibration, a reprocessing of the POLDER level-1 data is scheduled in the early months of 2001.

REFERENCES

[1] M. Shimada, H. Oaku, Y. Mitomi, H. Murakami, and H. Kawamura, "Calibration of the ocean color and temperature scanner," *IEEE transactions on geoscience and remote sensing*, vol. 37, pp. 1484-1495, 1999.

[2] P.-Y. Deschamps, F. M. Bréon, and A. P. M. Leroy, A. Bricaud, J.C. Buriez, and G. Sèze, "The POLDER Mission: Instrument Characteristics and Scientific Objectives," *IEEE Transactions on Geoscience and Remote Sensing*, vol. 32, pp. 598-615, 1994.

[3] Y. André, J. Laherrère, T. Bret-Dibat, M. Jouret, J. Martinuzzi, and J. Perbos, "Instrumental concept and performances of the POLDER instrument," presented at SPIE proc. Infrared spaceborne remote sensing III, San Diego, 1995.

[4] O. Hagolle, A. Guerry, L. Cunin, B. Millet, J. Perbos, J. M. Laherrère, T. Bret-Dibat, and L. Poutier, "POLDER Level 1 Processing Algorithms," presented at SPIE Aerosense proc. Algorithms For Multispectral And Hyperspectral Imagery II, Orlando, 1996.

[5] F. Cabot, G. Dedieu, and P. Maisongrande, "Monitoring NOAA/AVHRR and METEOSAT shortwave bands calibration and inter calibration over stable areas," presented at Proc. of the Sixth International Symposium on "Physical Measurements and Signatures in Remote Sensing", Val d'Isère, 1994.

[6] D. L. Smith, P. D. Read, and C. T. Mutlow, "Calibration of the visible/near-infrared channels of the Along Track Scanning Radiometer-2(ATSR-2)," presented at SPIE-EUROPTO conference on Sensors, systems and Next-Generation Satellites, London, UK, 1997.

[7] P. Henry, M. Dinguirard, and M. Bodilis, "Spot multi-temporal calibration over stable desert areas," presented at SPIE symposium on Aerospace and Remote Sensing, Orlando, 1993.

[8] O. Hagolle, P. Goloub, P.-Y. Deschamps, H. Cosnefroy, X. Briottet, T. Bailleul, J.M.Nicolas, F. Parol, B. Lafrance, and M. Herman, "Results of POLDER In-Flight Calibration," *IEEE Transactions on Geoscience and Remote Sensing*, vol. 37, pp. 1550-1566, 1999.

[9] H. Cosnefroy, M. Leroy, and X. Briottet, "Selection and characterization of Saharan and Arabian desert sites for the calibration of optical satellite sensors," *Remote Sensing of Environment*, vol. 58, pp. 101-114, 1996.

[10] F. Cabot, O. Hagolle, C. Ruffel, and P. Henry, "Use of remote sensing data repository for in-flight calibration of optical sensors over terrestrial targets," presented at Proc of SPIE'99, Denver, CO, USA, 1999.